Finite Element Parametric Study Involving the Effect of Cooling Channels on the Thermo-mechanical Behavior of a High Pressure Airplane Turbine Blade

Ricardo Pedro Arraial Mendes

ricardopmendes@gmail.com

Instituto Superior Técnico – Universidade de Lisboa, Portugal

November 2021

Abstract

With the competitiveness of the airline industry, aircrafts have to operate on tight schedules and extreme work conditions. Gas turbine engine components function under conditions of high temperatures, pressure and rotation speeds, with the high pressure turbine (HPT) experiencing some of the highest temperatures. To counter this, cooling mechanisms are introduced in order to lower the temperatures of the HPT blades and therefore assure their mechanical stability.

The objective of this work is to study the cooling mechanisms' influence on the temperature and deformation of an HPT blade. To do so, a blade model was created using the finite element method (FEM). To create the model, a blade scrap was obtained from a regional airline company. Also, a flight route operated by the same company was studied and information regarding the flight conditions of the turbine was retrieved from flight data records. A CAD 3D blade model from a similar engine was obtained, adapted and served as the basis of the FEM blade model created. After the data input, thermal and creep analyses were run on a rectangular block in order to validate the model, and were then performed on the blade model.

The simulations run were successful and, despite the assumptions and approximations made, the blade model offered reasonable results and proved itself a useful model in analyzing temperatures, displacements and predicting the deformation by the end of the blade's lifetime.

Keywords

High Pressure Turbine Blade, Finite Element Method, Creep, Temperature, Cooling, Deformation

1. Introduction

The aviation mode of transport has become increasingly more common and accessible in these current times. With the high competitiveness of the airline industry, aircrafts have to operate, on a daily basis, on tight schedules and under extreme work conditions. Gas turbine engine components function under very high temperatures, pressure and rotation speeds. The engine components that are under the most rigorous conditions are the combustion chamber and the high pressure turbine, with this section of the engine working under the influence of the highest temperatures in the engine. High pressure turbine blades usually operate at temperatures that could reach their constituting materials' maximum service temperature. To counter this effect, it is vital to introduce cooling mechanisms in order to lower the temperatures of the turbine blades and therefore assure their mechanical integrity [1] [2].

The main objective of this work is to study the cooling mechanisms' influence in the overall temperature of a turbine blade, as well as the effect that a temperature decrease can have on the overall deformation of the blade. This study gives sequence to a previous work where a predictive model of a blade without cooling channels was built in order to study the effects that the mechanical and thermal loads have on the turbine blades for several flight routes performed by a regional airline company that flies within the Azores islands and also between the island of São Miguel and the island of Madeira. To do so, in-flight information was retrieved from the Flight Data Record (FDR) for several flight routes.

The contribution of this study is the creation of a new blade model, using the finite element method (FEM), in which the cooling mechanisms' influence is considered. To create the FEM blade model, a CAD 3D blade model from a different engine was adapted until its dimensions were very similar to those of a turbine blade scrap obtained from the airline company. The PDL-FNC (São Miguel Island – Madeira Island) flight route was the object of the study, and its FDR data (temperatures and rotation speeds) was retrieved from the former study, as well as the blade material's properties.

In order to study how the cooling can influence the blade's temperature and deformation, thermal and creep analyses were performed using the finite element software ABAQUS, with the thermal analyses being run using two different approaches. Both the thermal and creep analyses were initially tested and validated in several rectangular block models with similar dimensions to the blade. With both the thermal and creep analyses properly defined in the blade model, a study on the accumulation of flight cycles was performed in order to predict the deformation of the blade by the end of its lifetime.

2. Materials and Methods

2.1. HPT Blade and Rectangular Blocks

The study of an HPT blade is crucial in order to understand how it deforms throughout a flight and also to predict the extent of the deformation by the end of its lifetime. For this effect, it was necessary to build a blade model using the finite element method in order to run simulations that would provide results that could be analyzed. To build this model, an HPT blade was acquired and its dimensions can be seen in **Figure 2.1 a)**.

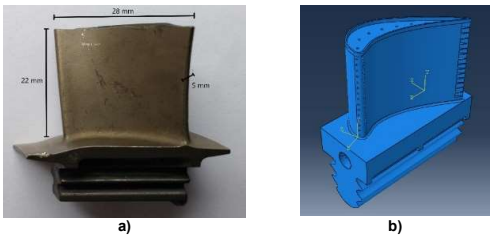

a) b)

Figure 2.1 - a) Discarded turbine blade dimensions; b) Adapted turbine blade model

Knowing these dimensions, a CAD drawing of a proportionately similar HPT blade from a different engine was acquired and adapted until their dimensions were very close. This adapted blade model can be seen in **Figure 2.1 b)**.
With the intention of building and studying the blade model, a rectangular block model (**Figure 2.2 a)**) was created with the dimensions of the HPT blade, in order to test the simulations and validate the finite element model built using the ABAQUS finite element software, that would later on be applied on the blade model.

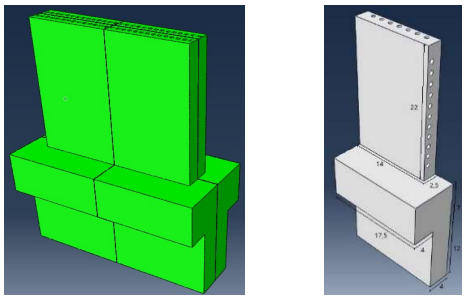

a) b)

Figure 2.2 - a) Rectangular block; b) Symmetrical rectangular block (B3-7L/11T) with dimensions

Given that the rectangular block is symmetrical in two axis, it was decided to study one quarter of the rectangular block in order to have a more refined finite element mesh, and therefore more precise results. This symmetrical rectangular block and its dimensions can be seen in **Figure 2.2 b)**.
To study the effect of the cooling mechanisms on temperatures and deformation, it was of interest to design several symmetrical block geometries with different numbers, sizes, orientations and locations of cooling channels, with the goal of studying the effect of the cooling flow that passes through the cooling channels on the temperatures and deformation of the several blocks. The description of these blocks is in **Table 2.1**.

Table 2.1 - Description of the symmetrical rectangular block geometries

B0	No cooling channels
B1-7L	7 longitudinal cooling channels
B2-14L	14 longitudinal cooling channels
B3-7L/11T	7 longitudinal / 11 transversal cooling channels
B4-11L/17T	11 longitudinal / 17 transversal cooling channels
B5-11L/11L	11 longitudinal / 11 longitudinal cooling channels
B6-11L/17T-Net	11 longitudinal / 17 transversal cooling channels in a net-like disposition

2.2. Material Properties and Flight-cycle Conditions

In the study that this work gives sequence to, the blade was analyzed, through reverse engineering, in order to determine its density and chemical composition, with the finality of choosing a material to characterize the blade, as that information was unavailable. That choice fell on the TMS-75 superalloy, and its thermal, mechanical properties and temperature and stress dependent plastic strains characterized the material used in the FEM block/blade model [1].
To simulate the in-flight conditions that the HPT blade goes through during the duration of a flight-cycle, information was obtained from flight data records (FDR) for the PDL-FNC flight route [1]. This resulted in the plots for the turbine-inlet-temperature (TIT) and the rotation speed (ω_{HPT}), which can be seen, in **Figures 2.3** and **2.4**, respectively.

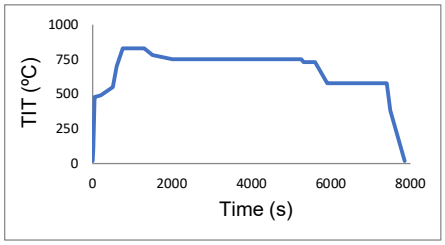

Figure 2.3 - Turbine Inlet Temperature (TIT) for a PDL-FNC flight cycle [1]

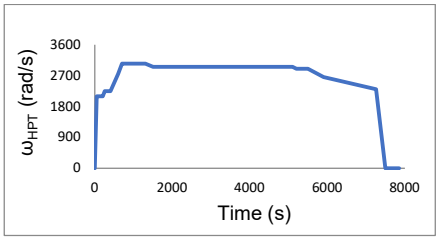

Figure 2.4 - Rotation speed - ωHPT for a PDL-FNC flight cycle [1]

To characterize the cooling flow, information had to be obtained regarding its temperature and convection coefficients. The temperature of the cooling flow is the exterior atmospheric temperature (EAT). To know the evolution of the EAT, it was necessary to first know the evolution of the altitude. However, given that access to the FDR records was unavailable, it was necessary to make an approximation. Comparing the PDL-FNC flight settings – ground speed, maximum flight altitude – with the settings of other similar flights, an altitude plot was adapted, and from it, calculations were made and an EAT plot was obtained, as can be seen in **Figure 2.5**.

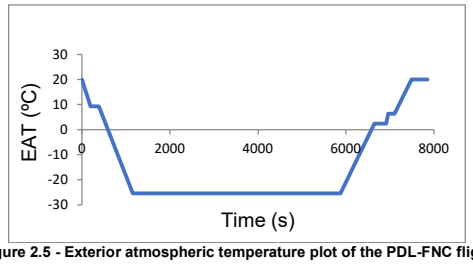

Figure 2.5 - Exterior atmospheric temperature plot of the PDL-FNC flight

2.3. Thermal Loading

As for the cooling channels' flow convection coefficients, two were considered in this study. The first one was assumed to be 500 W/m^{2}K, as the channels' cooling flow can be considered a high pressure gas inside tubes [3]. A second one was obtained from calculations made considering the diameter of the cooling channels [4]. The FEM simulations were run using both coefficients and their results were compared in order to assess the influence of the convection coefficient value on the temperature and deformation of both the block and blade models. Both convection coefficients can be consulted in **Table 2.2**.

Table 2.2 - Thermal analysis cooling channels' flow convection coefficients [3] [4]

Cooling flow convection coefficients, h (W/m^{2}K)	
First convection coefficient	**Second convection coefficient**
500	923

For the heating of the block/blade, two heating approaches were followed. The first one defines the TIT plot as the temperature of the outside walls of the blocks/blade during the duration of the flight cycle. In this approach, the temperature is defined as the boundary condition (temperature as boundary condition – TBC) as seen in **Figure 2.6 b)**. In **Figure 2.6 a)**, it is possible to see the cooling flow applied as a surface film condition on the cooling channels.

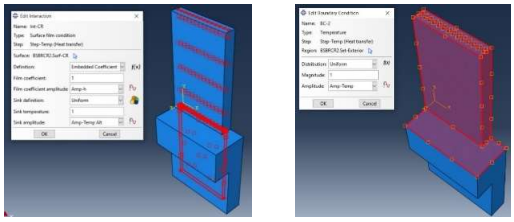

a) b)

Figure 2.6 – a) Cooling flow applied on the cooling channels as a surface film condition; b) Temperature applied as a boundary condition on the block's walls (TBC)

The second heating approach defines the TIT temperature plot as the temperature of a heating flow applied on the walls of the blocks/blade during the duration of the flight cycle. In this approach, the heating of the block/blade is provided by convection heat transfer, and therefore convection is the boundary condition (CBC). In this approach, the TIT temperature plot has to be affected by a multiplying factor (different in all geometries) in order to compensate for a significant drop of the block's temperatures when using the original TIT plot.
In the CBC approach, an additional cooling flow was applied on the outside surfaces. This surface film cooling flow originates from the cooling channels through tip cap cooling holes and film cooling holes and forms a protective surface film that envelops the block/blade's surfaces and reduces the influence of the heating flow, which is to say, the hot gases from the combustion chamber [2] [5]. Both the film cooling flow and the heating flow are applied on the walls as a surface film condition as seen in **Figure 2.7**.

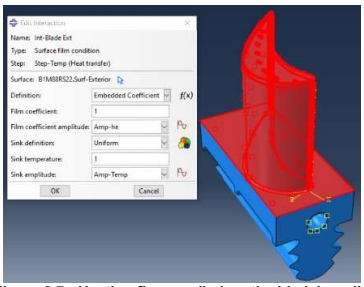

Figure 2.7 - Heating flow applied on the blade's walls

Like the cooling channels' flow, two convection coefficients were used for the surface film cooling flow. These were assumed to be approximately half of the cooling channels' flow, as information about the surface film cooling flow convection coefficient is scarce. This was assumed due to the fact that when the surface film cooling flow exits the cooling channels, it bears the impact of the heating flow, which could reduce its velocity and convection coefficient.
Both sets of cooling flow convection coefficients can be consulted in **Table 2.3**.

Table 2.3 - CBC thermal analysis cooling flow convection coefficients

Cooling flow convection coefficients (W/m^{2}K)			
First set of convection coefficients		**Second set of convection coefficients**	
Cooling channels' flow [h]	**Surface film flow [hc]**	**Cooling channels' flow [h]**	**Surface film flow [hc]**
500	250	923	450

When it comes to the heating flow, like the cooling flows, two sets of convection coefficients were used. The first set presented a coefficient of 500 W/m^{2}K for all surfaces of the block/blade [3]. The second set presented a more realistic approach, as a different convection coefficient was assigned to each surface of the block/blade Both sets for the different block/blade surfaces can be consulted in **Table 2.4**.

Table 2.4 - CBC thermal analysis heating flow convection coefficients [6]

	Heating flow convection coefficients (W/m^{2}K)	
	First set [he]	**Second set [hev]**
Convex surface	500	1265 [hecx]
Concave surface	500	975 [hecv]
Tip surface	500	840 [het]
Platform surface	500	839 [heb]

2.4. Mechanical Loading and Mesh

With the thermal loading defined, the next step would be to apply the mechanical loading on the block/blade model. After the application of the boundary conditions on the base of the block/blade – symmetry in the XX axis and symmetry and pinned in the ZZ axis – the rotation speed plot was applied as a rotational body force around an axis of rotation as can be seen in **Figure 2.8**.

With both loadings defined, the final step in the construction of the FEM model would be to build a finite element mesh. For the thermal analysis, a standard heat transfer DC3D10 element was used, and for the creep analysis, a standard 3D stress C3D10 element. Both elements present a seed size element of 1 mm.

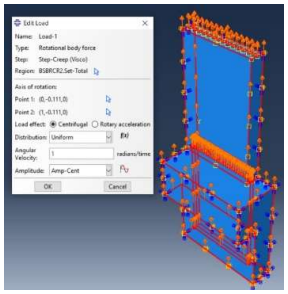

Figure 2.8 - Centrifugal load applied on the block model

3. Results and Discussion

3.1. Rectangular Block

To properly evaluate the numerical results and compare them between different block geometries, six points were chosen for which results were calculated. Points 1-4 were chosen due to their location at the top of the symmetrical blocks, where the displacements relevant to this study take place. Points 5T and 6T are temperature points. These points can be viewed in **Figure 3.1**.

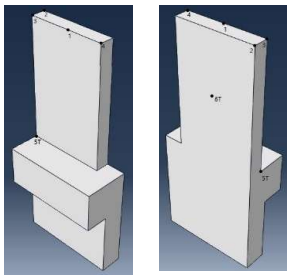

Figure 3.1 - Points selected for the symmetrical block

3.1.1. Thermal Analysis Results – TBC

The study of the temperature distribution on the several rectangular blocks was made at a time instant of approximately 3000 s, due to it belonging to the aircraft's cruise flight phase, the longest period of time during the flight in which the TIT remains a constant. For the first convection coefficient of h=500 W/m^{2}K, results for the B2-14L geometry were obtained and can be viewed in **Figure 3.2**.

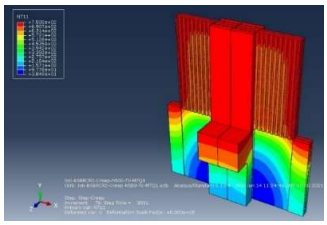

Figure 3.2 - Temperature distribution for the B2-14L rectangular block geometry (TBC)

From its observation one can easily see that a cooling effect is taking place. The block's walls are at 750 ºC which is the TIT for the chosen instant of time. The interior of the block is at lower temperatures than the walls' temperature, proving that the cooling channels and cooling flow are having the desired effect on the block's temperature distribution. The numerical results were collected on point 6T for all block geometries and they can be consulted in **Table 3.1**.

Table 3.1 - Temperature results for the rectangular block geometries (TBC)

Rect. Block Geometry	Cooling Channels' Surface Area (m^2)	Temperature (ºC)	
		Wall Temperature	Point 6T
B0	0	750	750
B1-7L	4.836E-04	750	692.5
B2-14L	6.770E-04	750	673.8
B3-7L/11T	6.770E-04	750	669.1
B4-11L/17T	8.440E-04	750	656.9
B5-11L/11L	8.511E-04	750	657.3
B6-11L/17T-Net	7.985E-04	750	674.1

The block geometries with cooling channels present a general decrease in temperature when there's a corresponding increase of the number of cooling channels. Considering the cooling channels distribution, the geometries that contain a mixture of separated longitudinal and transversal channels present lower temperature results when compared to geometries with solely longitudinal channels.
With the increase of the cooling channels' surface area, there is consequentially a larger interaction between the cooling flow and the blocks, and the results in most cases indicate that there is a decrease of temperature with the increase of the cooling channels' surface area.
To conclude the TBC thermal analysis, a simulation of the B2-14L geometry was made using a cooling flow with the second convection coefficient of h=923 W/m^{2}K. These results and their comparison to previous results can be seen in **Table 3.2**.

Table 3.2 - Temperature results for the B2-14L geometry for h=500 W/m^{2}K and h=923 W/m^{2}K (TBC)

Rectangular Block Geometry	h (W/m^{2}K)	Temperature (ºC)	
		Wall Temperature	Point 6T
B2-14L	500	750	673.8
B2-14L	923	750	614.8

The temperature results of point 6T are clear in pointing out that a significant increase in the convection coefficient led to a decrease in temperature.

3.1.2. Thermal Analysis Results – CBC

After applying the heating flow and surface film cooling flow on the block's walls, the analysis was submitted and the temperature distribution results for B2-14L may be viewed in **Figure 3.3**.

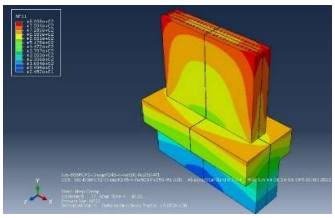

Figure 3.3 - Temperature distribution for the B2-14L geometry (CBC)

Through the graphical analysis of **Figure 3.3**, the first noticeable factor is that the temperature distribution of the CBC thermal analysis is quite different than the one of the TBC thermal analysis. The highest temperatures are localized at the upper edges of the leading and trailing edge and the lowest surface temperatures can be found mid-block and at the bottom which can be explained by the

fact that the lower section of the block is being more affected by the cooling flow of the cooling channels.
As for the numerical results, they can be viewed in **Table 3.3**.

Table 3.3 - Temperature results for the rectangular block geometries (CBC)

h=500 W/m²K; h=500 W/m²K; hc=250 W/m²K					
Rect. Block Geometry	Temp. (K) Multip. Factor	Temperature (ºC) (t ≈ 3000 s)			Temp. Difference (ºC)
		Point 4 (High Temp. Point)	Point 3 (Approx. 750 ºC)	Point 5T (Low Temp. Point)	Point 4 – Point 5T
B0	1.39	757.5	757.5	757.5	0
B1-7L	2.2	857.2	766.8	544.2	312.9
B2-14L	2.45	869.8	759.9	568.5	301.3
B3-7L/11T	2.3	854.8	760.5	569.5	285.3
B4-11L/17T	2.53	870.7	760.4	582.8	288
B5-11L/11L	2.63	891.9	760.3	530.2	361.7

Numerically, due to the effect of a different multiplying factor for all geometries, the comparison of point temperature results can't be made directly and so, the different temperature gradients were compared. These temperature gradients are a result of the effect that the combination of both the heating flow and cooling flows are having on the block. Taking this into account, it is possible to assume that a lower temperature gradient can provide an indication of a closer equilibrium between the heating flow and the cooling flows.
By analyzing and comparing these temperature gradients, it is possible to observe that the geometries that present lower temperature gradients are the ones that possess both longitudinal and transversal cooling channels, as seen before in the TBC thermal analyses.

3.1.3. Creep Analysis Results – TBC

After running the TBC thermal analysis, their temperature results were inserted in the TBC creep analysis. To analyze the creep results, the instant of time at which the block/blade is uniformly at the room temperature of 20 ºC was chosen. This time instant occurs after the flight cycle time and cooling time has taken place. With that said, it is important to define the time periods relevant for this study.
The first time period to consider is the Flight Cycle Time. A flight cycle begins when the engine is started before takeoff, and ends after the airplane lands, when the engine is shut down. For the PDL-FNC flight considered in this study, the flight cycle takes 7492 seconds from beginning to end [1]. At this time instant (engine shutdown), the rectangular block is still at very high temperatures and the cooling flow ceases to be in effect and so all block cooling will be achieved by natural convection and conduction.
The second time period relevant to the analysis is the Surface Cooling Period. This period represents the time it takes for the wall temperature to reach the room temperature, 20 ºC. This period was considered to be 363 seconds, and so the block's walls are at 20 ºC at the 7855 time instant [1].
The third and final time period is the Uniform Cooling Period. This time period corresponds to the time necessary for the rectangular block to uniformly achieve the room temperature of 20 ºC.

The time instants corresponding to these three time periods can be consulted in **Table 3.4**, for all block geometries.

Table 3.4 - Flight Cycle Time and Cooling Periods for the rectangular block geometries (TBC)

h = 500 W/m²K			
Rectangular Block Geometry	Flight Cycle Time (s)	Flight Cycle Time with Surface Cooling Period (s)	Flight Cycle Time with Surface and Uniform Cooling Periods (s)
B0	7492	7855	8763
B1-7L	7492	7855	8699
B2-14L	7492	7855	8681
B3-7L/11T	7492	7855	8715
B4-11L/17T	7492	7855	8722
B5-11L/11L	7492	7855	8639
B6-11L/17T-Net	7492	7855	8691

Knowing the time instants at which the whole block is at 20 ºC, the variable representing the displacement in the longitudinal direction (U2) was obtained. The U2 displacement distribution for the B2-14L geometry can be seen in **Figure 3.4**.

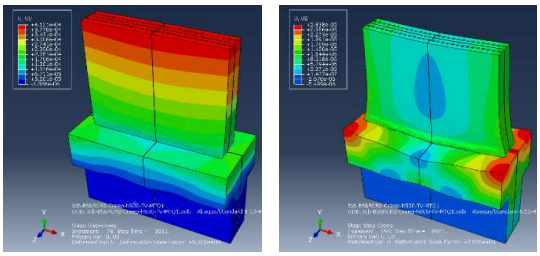

a) b)

Figure 3.4 - Displacement in the longitudinal direction U2 distribution for the B2-14L block geometry at a) t = 3031 s – cruise flight phase; b) t = 8681 s – after the uniform cooling period (TBC)

By looking at the U2 displacement distributions at both time instants, it is possible to see that during the cruise flight phase (**Figure 3.4 a)**), due to the effect of the turbine's high rotation speed, and facilitated by the hot gas high temperatures, the block is driven forward in the longitudinal direction, and in this stage of the flight, some of the highest displacement values during the flight cycle are registered.
As for the displacement distribution by the end of the flight cycle and cooling period (**Figure 3.4 b)**), it is possible to observe that the middle-block/top section registers the lowest displacement values of the block, which can be explained by the fact that it experiences some of the lowest temperatures during the flight, due mainly to the influence of the cooling flow. The surrounding section, which includes the trailing and leading edge, presents the highest values of U2 displacement of the block. This can also be justified by the cooling flow, which has a smaller influence on this section.

The numerical results obtained for points at the top of the block are presented in **Table 3.5**.

Table 3.5 - Creep analysis results of the displacement in the longitudinal direction U2 for the rectangular block geometries (TBC)

h = 500 W/m²K				
Rect. Block Geometry	U2 (m)			
	Point 1	Point 2	Point 3	Point 4
B0	8.749E-05	8.578E-05	8.570E-05	9.065E-05
B1-7L	9.963E-06	7.918E-06	7.894E-06	1.400E-05
B2-14L	5.379E-06	3.305E-06	3.255E-06	9.332E-06
B3-7L/11T	1.930E-05	1.738E-05	1.733E-05	2.305E-05
B4-11L/17T	1.494E-05	1.298E-05	1.293E-05	1.871E-05
B5-11L/11L	8.462E-06	6.448E-06	6.383E-06	1.257E-05
B6-11L/17T-Net	1.182E-05	9.865E-06	9.800E-06	1.560E-05

From the analysis of the results, it is possible to see that for all geometries the displacement values of point 4 are the highest, as this point is located at the leading and trailing edge, where the temperatures are highest and the cooling flow isn't as influential. On the other hand, points 2 and 3, being positioned mid-block exhibit the lowest displacement values.
When directly comparing point results for different geometries, it becomes clear that the block geometries with both longitudinal and transversal cooling channels present higher values of U2 displacement, while geometries with solely longitudinal channels display lower displacement values, with the B2-14L geometry being the one that displays the lowest values for all points. This is unexpected when considering that the B3-7L11T, B4-11L/17T geometries presented higher levels of cooling efficiency when compared to the geometries with strictly longitudinal cooling channels. Possible reasons to explain this behavior can be found by studying the B2-14L geometry, given that it displays the lowest U2 displacement values.
The B2-14L geometry presents the highest number of longitudinal cooling channels in a single line. Therefore, it is possible to assume that, locally, at the top of the block, the cooling efficiency improves with the increase of the number of cooling channels. So, even though globally the B4-11L/17T geometry has a higher cooling efficiency, as seen in the thermal analysis study, locally, at the top of the block, the B2-14L geometry presents lower U2 displacement results.
To finalize the study of the TBC creep analysis, a simulation of the B2-14L geometry was made but with the change of the cooling flow's convection coefficient to h=923 W/m²K. These results can be consulted in **Table 3.6**.

Table 3.6 - Creep analysis results of the displacement in the longitudinal direction U2 for the B2-14L block geometry when h=500 W/m²K and h=932 W/m²K geometry (TBC)

Rectangular Block Geometry	h (W/m²K)	U2 (m)			
		Point 1	Point 2	Point 3	Point 4
B2-14L	500	5.379E-06	3.305E-06	3.255E-06	9.332E-06
B2-14L	923	1.828E-06	-6.044E-08	-6.660E-08	5.359E-06

Looking at the results obtained by both analyses, it becomes apparent that the increase of the convection coefficient of the cooling flow led to a considerable reduction of the U2 displacement values, even to the point of contraction, as seen in points 2 and 3.

3.1.4. Creep Analysis Results – CBC

This second creep analysis was made using the CBC thermal analysis results.
As for the time periods relevant to the study, the Flight Cycle Time naturally remains the same, as the flight time has not changed. The second time period, the Surface Cooling Period, also remains the same, though in this case the Surface Cooling Period was enforced to decrease the heating flow temperature until the atmosphere surrounding the blades was at 20 ºC. As for the third time period, the Uniform Cooling Period, in the case of the CBC analysis, is considerably higher than the one necessary in the TBC analysis. This time discrepancy between both thermal analysis is explained by the fact that in the TBC analysis the wall temperature is forced to be at 20 ºC at the end of the Surface Cooling Period, which in turn will accelerate the cooling of the internal block. In the CBC analysis what reaches 20 ºC at the end of the Surface Cooling Period is the heating flow temperature. This will allow for a longer period of heat transfer between the block and the surrounding atmosphere at 20 ºC. A longer Surface Cooling Period though, seems to be much more consistent with reality, as an airplane engine can take approximately 2 to 4 hours to completely cool down to room temperature [7]. It is therefore possible to affirm that the CBC thermal analysis in which convection is the boundary condition is a more realistic approach to the heating and cooling dynamics of a turbine blade.
The time periods for all block geometries can be consulted in **Table 3.7**.

Table 3.7 - Flight Cycle Time and Cooling Periods for the rectangular block geometries (CBC)

h=500 W/m²K ; he=500 W/m²K ; hc=250 W/m²K			
Rectangular Block Geometry	Flight Cycle Time (s)	Flight Cycle Time with Surface Cooling Period (s)	Flight Cycle Time with Surface and Uniform Cooling Periods (s)
B0	7492	7855	21529
B1-7L	7492	7855	13736
B2-14L	7492	7855	13565
B3-7L/11T	7492	7855	14118
B4-11L/17T	7492	7855	13748
B5-11L/11L	7492	7855	12165
B6-11L/17T-Net	7492	7855	13915

The displacement distribution for the B2-14L geometry can be seen in **Figure 3.5** and the numerical results for the points at the top of the block can be viewed in **Table 3.8**.

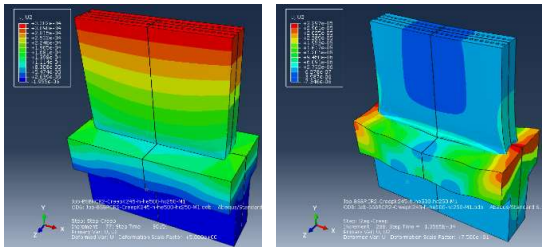

a) b)

Figure 3.5 - U2 displacement distribution of the B2-14L block geometry for a) t=3015 s – cruise flight phase; b) t=13565 s – after the uniform cooling period (CBC)

Table 3.8 - Creep analysis results of the displacement in the longitudinal direction U2 for the rectangular block geometries (CBC)

h=500 W/m²K ; he=500 W/m²K ; hc=250 W/m²K				
Rectangular Block Geometry	U2 (m)			
	Point 1	Point 2	Point 3	Point 4
B0	7.596E-05	7.432E-05	7.424E-05	7.901E-05
B1-7L	2.982E-06	1.665E-06	1.654E-06	5.780E-06
B2-14L	-4.173E-07	-1.600E-06	-1.603E-06	2.013E-06
B3-7L/11T	1.574E-05	1.464E-05	1.463E-05	1.813E-05
B4-11L/17T	1.185E-05	1.078E-05	1.078E-05	1.416E-05
B5-11L/11L	3.844E-07	-5.302E-07	-5.567E-07	2.670E-06
B6-11L/17T-Net	4.161E-06	2.953E-06	2.932E-06	6.653E-06

Just like in the TBC creep analyses, it is perceivable for all geometries, that points 2 and 3 exhibit the lowest displacement values – even to the point of contraction - whereas point 4 presents the highest, like in the TBC creep analysis.

Finally, comparing both methods of creep analysis, it is clear that the CBC creep analysis presents lower U2 displacement values for all points and geometries. This can be justified by the longer cooling period which leads to a longer period of contraction for the block, and consequently, lower U2 displacements.

To finalize the study of the rectangular blocks, CBC creep analyses were run for the B2-14L and B3-7L/11T geometries when using the second set of convections coefficients. The results of these analyses and their comparison to previous results can be viewed in **Table 3.9**.

Table 3.9 - Creep analysis results of the displacement in the longitudinal direction U2 for the B2-14L and B3-7L/11T geometries with two sets of convection coefficients (CBC)

Rect. Block Geom.	(W/m²K)			U2 (m)			
	h	he	hc	Point 1	Point 2	Point 3	Point 4
B2-14L	500	500	250	-4.1E-07	-1.6E-06	-1.6E-06	2E-06
B2-14L	923	hev	450	-4.6E-06	-5.7E-06	-5.6E-06	-2.3E-06
B3-7L/11T	500	500	250	1.6E-05	1.4E-05	1.4E-05	1.8E-05
B3-7L/11T	923	hev	450	9.8E-06	8.7E-06	8.7E-06	1.2E-05

For both geometries, it is clear that the usage of the second set of convection coefficients leads to a higher level of contraction at the top of the blade, when compared to the first set of convection coefficients - in fact, all point values at the top of the block exhibit contraction displacements. This is justified by the increase of the cooling channels' cooling flow and the surface film cooling flow convection coefficients. Despite the increase of the heating flow coefficients for all surfaces of the block, the influence of both cooling flows is more than enough to override this added heating effect.

In conclusion, all the analyses run on the rectangular blocks delivered consistent results for the U2 displacement variable, based on the expected influence of cooling efficiency on creep deformation. Hence, having these thermal and creep models running consistently on the rectangular block, they could now be applied to the turbine blade model.

3.2. Turbine Blade

Before proceeding to the thermal and creep analyses of the turbine blade, it was first necessary to choose study points for which results could be obtained. For this effect six points were chosen, four at the top of the blade, points 1 through 4, and two mid-blade, points 5T and 6T which are purely thermal points. Their location can be seen in **Figure 3.6**.

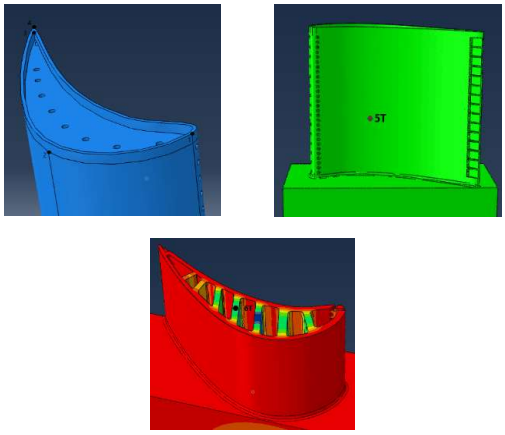

Figure 3.6 - Points selected for the turbine blade

3.2.1. Thermal Analysis Results – TBC

After validating the thermal and creep analyses on the rectangular block, the same analyses in the same conditions were performed on the turbine blade. The temperature distributions of the turbine blade using h=500 W/m²K can be viewed in **Figure 3.7**.

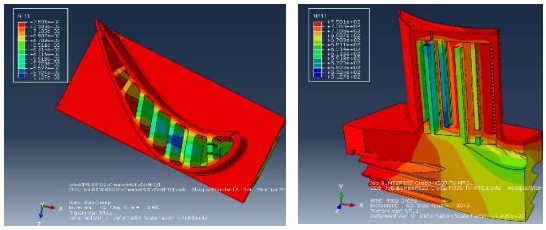

Figure 3.7 - Temperature distribution of the turbine blade using a convection coefficient of h=500 W/m²K at t=3040 s (TBC)

From the observation of the temperature distributions, it is clear that the cooling flow is effectively cooling down the interior of the blade. The blade's walls are at 750 ºC, as expected per the instant of time. At the same time, the interior of the block registers the lowest temperatures due to the effect of the cooling flow.
Looking at the middle of the blade, one can observe that there is a section in which the temperatures are at its lowest (blue) – this can be explained by the fact that this fin is located in the section in which the width of the blade is the largest. This means that the middle of the fin is farthest from the blade walls, which is the hottest section of the blade, while at the same time being closest to the cooling flow. In fact, it is possible to conclude that with the reduction of the width of the blade, comes a consequential and gradual increase of the temperature of the internal fins.
As for the numerical results for both cooling flow convection coefficients, they can be viewed in **Table 3.10**.

Table 3.10 - Temperature results for the turbine blade when h=500 W/m²K and h=923 W/m²K (TBC)

h (W/m²K)	Time (s)	Temperature (ºC)	
		Wall Temperature	Point 6T
500	3040	750	576.8
923	3020	750	459.7

For both cooling coefficients, it is easy to conclude that the cooling flow is having its effect as this temperature is significantly lower than the wall temperature. Also, when comparing the results of both convection coefficients, it is clear that the increase of the convection coefficient value

resulted in a decrease of temperature, due to the added cooling capacity of the cooling flow.

3.2.2. Thermal Analysis Results - CBC

The second thermal analysis run was the CBC analysis, also in the same conditions as the one for the rectangular block. The temperature distribution of the turbine blade for the first set of convection coefficients can be viewed in **Figure 3.8**.

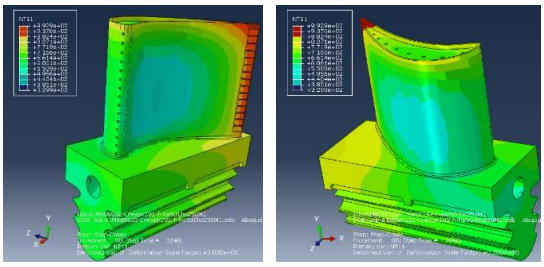

Figure 3.8 - Temperature distribution of the turbine blade for the first set of convection coefficients at t=3040 s (CBC)

Through the analysis of **Figure 3.8**, it is noticeable that a cooling effect is taking place. This effect is visible in both the convex and concave sections of the blade. It is also possible to observe that the edges of the tip of the blade, and the areas closest to the trailing edge exhibit high temperature values, due to the effect of the heating flow, but it's the trailing edge that registers the highest temperatures of the blade. This can be explained by the fact that the trailing edge has the smallest width of the blade, and therefore is less subjected to the internal cooling flows while at the same time being under the direct effect of the heating flow. In contrast, the sections with the largest width of the blade present the lowest temperatures, as seen in the convex and concave surfaces – this can be justified by the cooling flow injecting an increased amount of cold air mass that fills up the hollow spaces of the widest sections of the blade, which in turn will produce a higher cooling effect as it increases the heat transfer rate.
The temperature results of the analyses, using the two sets of convection coefficients can be observed in **Table 3.11**.

Table 3.11 - Temperature results for the turbine blade with two sets of convection coefficients (CBC)

(W/m^2K)			Temperature (ºC) (t ≈ 3000 s)			Temp. Difference (ºC)
h	he	hc	Point 4 (High Temp. Point)	Point 2 (Approx. 750 ºC)	Point 5T (Low Temp. Point)	Point 4 – Point 5T
500	500	250	992.9	755.7	487.1	505.8
923	hev	450	929.5	754.5	450.9	478.6

From the results, one can conclude that using the second set of convection coefficients resulted in the reduction of the temperature values for all points considered, as expected. This will lend itself to lower U2 displacement values, as will be seen in the creep analyses.

3.2.3. Creep Analysis Results – TBC

The first creep analysis of the turbine blade model was conducted using the TBC thermal analysis results under the same conditions.
As for the time periods considered in this study, both the Flight Cycle Time and Surface Cooling Period remain the same. The Uniform Cooling Period will, naturally, be different, as the rectangular block geometry and the blade are very different in shape. The turbine blade's cooling time periods for the TBC creep analysis can be consulted in **Table 3.12**.

Table 3.12 - Flight Cycle Time and Cooling Periods of the turbine blade (TBC)

h (W/m^2K)	Flight Cycle Time (s)	Flight Cycle Time with Surface Cooling Period (s)	Flight Cycle Time with Surface and Uniform Cooling Periods (s)
500	7492	7855	8790
923	7492	7855	8820

Knowing the time periods and the time instant at which the whole blade is at 20 ºC, the U2 displacement distributions could then be obtained. These results can be viewed for the first convection coefficient in **Figure 3.9.**

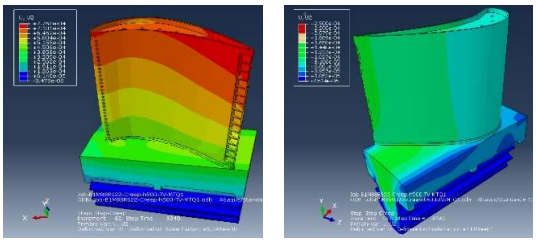

a) **b)**

Figure 3.9 - U2 displacement distribution of the turbine blade when h=500 W/m^2K for a) t=3040 s (cruise flight phase) b) t=8790 s (20 ºC uniform temperature) (TBC)

Observing the displacement distribution at the end of the cooling periods, two main sections of deformation can be established: the first section contains most of the leading edge, the leading end of the convex surface and the leading end of the concave surface; the second section contains the trailing edge and its close proximities.
The first section exhibits the lowest U2 displacement values of the blade, due to this section possessing the largest widths of the blade. On the opposing side of the blade, the second section exhibits the highest U2 displacement values of the blade, as it presents the lowest widths of the blade and, therefore, is less influenced by the cooling flow while being affected by the walls' temperature.
To confirm the conclusions taken from the graphical results, a study of the numerical results was made. These results can be found in **Table 3.13**.

Table 3.13 - Creep analysis results of the displacement in the longitudinal direction U2 of the turbine blade (TBC)

h (W/m^2K)	U2 (m)			
	Point 1 Leading edge	Point 2 Center Convex Surf.	Point 3 Trailing edge	Point 4 Trailing edge tip
500	7.936E-05	7.136E-05	1.071E-04	1.082E-04
923	7.621E-05	6.728E-05	1.012E-04	1.023E-04

The first observation from the results, is that the lowest U2 displacement can be found on the center of the convex surface (point 2) – this is due to its positioning at the widest section of the blade.
As for the highest U2 displacement, it can be observed on the trailing edge tip (point 4) – this is due to its location on the blade where its width is the lowest.
These observations are valid for both analyses with different convection coefficients. The main difference between the analyses is that, as expected, the analysis in which the higher convection coefficient was used delivered lower displacement values for all points.

3.2.4. Creep Analysis Results – CBC

The second creep analysis was conducted using the CBC thermal analysis results, under the same conditions. As for the time periods, they can be consulted in **Table 3.14**.

Table 3.14 - Flight Cycle Time and Cooling Periods of the turbine blade (CBC)

h (W/m^2K)	Flight Cycle Time (s)	Flight Cycle Time with Surface Cooling Period (s)	Flight Cycle Time with Surface and Uniform Cooling Periods (s)
500	7492	7855	17490
923	7492	7855	17381

Like the CBC creep analysis of the rectangular block geometry, it is possible to observe that the Uniform Cooling Period is significantly larger than the one observed in the TBC creep analysis.
With the knowledge of the Flight Cycle Time with both cooling periods, the U2 displacement distribution could then be obtained. These results can be viewed for both sets of convection coefficients in **Figure 3.10**.

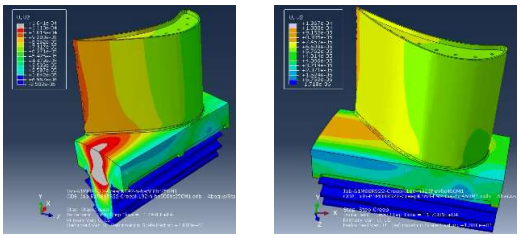

a) b)

Figure 3.10 - U2 displacement distribution of the turbine blade for the a) first set of convection coefficients; b) second set of coefficients (CBC)

From the observation of the CBC temperature distribution, it is possible to see that it follows similar patterns of deformation to the TBC creep analysis, with two main sections with the same behavior.
To confirm these observations, a study of the numerical results was made and it can be consulted in **Table 3.15**.

Table 3.15 - Creep analysis results of the displacement in the longitudinal direction U2 of the turbine blade (CBC)

h ; he ; hc (W/m^2K)	U2 (m)			
	Point 1 Leading edge	Point 2 Center Convex Surf.	Point 3 Trailing edge	Point 4 Trailing edge tip
500 ; 500 ; 250	6.962E-05	6.253E-05	9.282E-05	9.369E-05
923 ; hev ; 450	6.356E-05	6.139E-05	7.530E-05	7.534E-05

From **Table 3.15** it is possible to observe that the lowest U2 displacement can be found in point 2, the center of the convex surface, as it is positioned where the blade's width is the largest. As seen before, the highest U2 displacement can be found where the width is the lowest, which is point 4, the trailing edge tip.
As for the influence of both sets of convection coefficients, it can be concluded that using the second set produces lower displacement values for all points.
To finalize the CBC creep analysis study, it is possible to conclude that the U2 displacement values obtained when performing the CBC analysis are lower than those obtained when performing the TBC creep analysis, due to the longer cooling periods.

3.2.5. Cycle Accumulation Study

One of the objectives of this study was to predict how much the turbine blade deforms throughout its lifetime. So far, this work has been focused on the U2 displacement results for a single flight cycle with cooling periods. Therefore, in order to properly make a prediction of the deformation the blade endures, it was necessary to acquire information regarding the blade's lifetime, the aircraft's turnaround time for the PDL-FNC flight cycle, and the rest time after a day's work.
In the work of which this study is a continuation, it was possible to find that the duration of the blade's lifetime is 3000 flight hours [1]. Knowing that a PDL-FNC flight cycle takes 7492 s, it is possible to conclude that the HPT blade can perform for 1442 flight cycles (C) before having to be replaced.
In order to base this study in reality as much as possible, the turnaround time information was obtained - for the flight in question, it is approximately 1800 s. With the knowledge of both the flight cycle time and the turnaround time, it was defined that each cycle studied would begin at the start of the flight cycle time and would close at the end of the turnaround time.
As for the rest time, during peak season, an airplane can register up to 11/12 flight hours a day – approximately 6 PDL-FNC flight cycles. Therefore, the rest time can be assumed to be in the vicinity of 10 hours a day (36000 s). However, given computational limitations, the rest time (R) considered was 10400 s, which is a time period that allows for the complete cooling of the blade in the CBC analysis.
With this information, an analysis of 4 aircraft workdays and two extra cycles was made using the second set of convection coefficients. These analyses were both TBC and CBC creep analyses, and the U2 displacement results at the end of each cycle were obtained, as well as the U2 displacement trendlines. The results for the CBC creep analysis can be viewed in **Figure 3.11.**

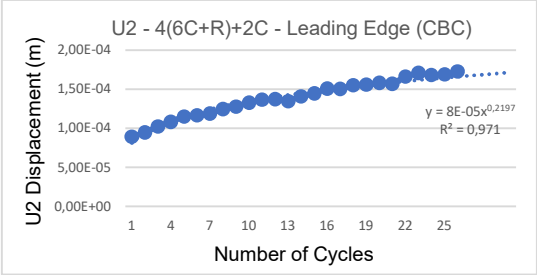

Figure 3.11 - Displacement (U2) and trendline of the leading edge for 4(6C+R)+2C (CBC)

With the trendlines obtained from the cycle analyses for all cycles, and knowing that the blade has a lifetime of 1442 cycles, a prediction of the deformation at the end of the blade's lifetime could be calculated. These results can be consulted in **Table 3.16**.

Table 3.16 - Displacement (U2) of the turbine blade for 1442 cycles based on the U2 trendlines (TBC and CBC)

Study Points	U2 (m) (1442 cycles)	
	U2 Trendlines - TBC	U2 Trendlines - CBC
	4(6C+R)+2C	4(6C+R)+2C
Point 1 - Leading Edge	3.225E-04	3.955E-04
Point 2 – Center of Convex Surface	1.182E-04	2.645E-04
Point 3 - Trailing Edge	2.658E-04	1.218E-04

Analyzing the results, it is possible to see that the U2 displacement values of the leading end of the blade are higher in the CBC creep analyses than the ones obtained

in the TBC creep analysis. However, when taking into account that in the TBC analysis the Uniform Cooling Period of the blade is inferior to the turnaround time, it is easy to understand that by the end of the turnaround time, the blade has achieved a uniform temperature of 20 ºC. On the other hand, for the CBC analysis, the Uniform Cooling Period is significantly larger than the turnaround time, and the blade is still at temperatures between 35 ºC and 51 ºC when the turnaround time ends and the airplane takes off again, beginning a new cycle. Therefore, in the TBC analysis the blade cools down faster and the contraction of the blade will also be superior. The rest time helps in attenuating this effect for the CBC analysis as it is possible to see in **Figure 3.11** that at the 7th cycle, and every 6 cycles, there is a drop or a stabilization of the U2 displacement.
Another observation is that now the leading edge presents the highest U2 displacement values. A possible explanation for why the trailing edge deforms less than the leading edge lies in the width of the blade. As the cycles keep accumulating, the small widths of the trailing edge, and therefore lack of significant internal space nearby, results in its favor. As the cycles add up, the trailing edge deforms at a lower rate than the leading end, with the results being that the leading end of the blade, by the end of its lifetime, has deformed more than the trailing edge, and so presents higher U2 displacement values.

Even though the results obtained are merely predictions, overall, one can conclude that the U2 displacement values by the end of the blade's lifetime can be considered very reasonable, as the blade has deformed, at most, less than half a millimeter (0.3955 mm). This seems to coincide with reality, as these blades are substituted by new ones at the end of their lifetime, before significant deformation occurs.

4. Conclusions

At the conclusion of this work, it is possible to state that a finite element model for temperature and deformation of a gas engine turbine blade taking into account different cooling modes was developed. Certain assumptions, approximations and simplifications had to be made though, as precise information regarding the blade's material and flow convection coefficients is difficult to come by. For this reason, rectangular blocks with several cooling channel configurations were studied, so as to establish the consistency of the proposed approach. This allowed the assumptions and approximations made to be considered reasonable, leading to results that both for block geometries and for a blade shape are fairly close to what could be expected in reality. The main conclusions that were taken from this work can be read below:

The B0 block geometry with no cooling channels displayed the highest U2 displacement results;

The B4-11L/17T block geometry proved to be the most efficient at reducing its internal temperatures - in general, block geometries with both longitudinal and transversal cooling channels exhibit lower internal temperatures, and therefore superior cooling efficiency than geometries with solely longitudinal cooling channels;

The B2-14L geometry displayed lower U2 displacement values when compared to the other geometries – in general, block geometries with solely longitudinal channels exhibited lower U2 displacements/higher contractions when compared to geometries with both longitudinal and transversal cooling channels;

With the increase of the cooling flow's convection coefficient, comes a decrease of the temperature of the block/blade and a decrease of the U2 displacements;

The CBC creep analysis, which utilizes the temperature results obtained by the CBC thermal analysis, seems to be a more realistic approach than the TBC creep analysis;

For one flight cycle and cooling periods, the blade exhibits its lowest U2 displacement values where its widths are the largest (with the center of the convex surface exhibiting the lowest displacement), and its highest U2 displacement values where its widths are the smallest (with the trailing edge exhibiting the highest displacement);

For one flight cycle and for the ranges of heat transfer coefficients that were analyzed, the U2 displacements for both the CBC and the TBC analysis are within the same order of magnitude;

By the end of the blade's lifetime, the leading edge displays the highest U2 displacements, and the trailing edge displays the lowest; these displacement results are in the sub-millimeter range and they are similar for both the CBC and the TBC analysis;

The cycle accumulation study provided a solid prediction of the blade's deformation by the end of its lifetime;

Overall, in conclusion, the rectangular block model provided a suitable model for the validating of the thermal and creep analyses, and the blade model offered reasonable results and proved itself a useful model in analyzing temperatures, U2 displacements and predicting the deformation by the end of the blade's lifetime. This highlights something that is well known, which is how important the cooling channels and cooling dynamics are in minimizing the deformation and maximizing the lifetime of the turbine blade.

References

[1] P. M. B. Brandão, "Thermo-mechanical Modeling of a High Pressure Turbine Blade of an Airplane Gas Turbine Engine", 2005.

[2] M. P. Boyce, "Axial-Flow Turbines," em *Gas Turbine Engineering Handbook*, 2nd ed., Woburn MA, Butterworth-Heinemann, 2002, pp. 351-363.

[3] Engineers Edge, "Overall Heat Transfer Coefficient Table Chart," Engineers Edge, [Online]. Available: https://www.engineersedge.com/thermodynamics/overall_heat_transfer-table.htm. [Accessed on October 2020].

[4] A. H. Ayaal, J. M. Jalil e K. K. Abbas, "Thermal Analysis of a Cooled Turbine Blade," em *2nd International Conference on Sustainable Engineering Techniques*, Baghdad, Iraq, 2019.

[5] D. G. Bogard e K. A. Thole, "Gas Turbine Film Cooling," em *J. Propuls. Power, vol 21, no. 6*, vol. 21, 2005, p. 24.

[6] G. Creci, M. Teixeira de Mendonça, J. C. Menezes e J. R. Barbosa, "Heat Transfer Analysis in a Single Spool Gas Turbine," *Applied Sciences,* 24 November 2020.

[7] Quora, "How long does it take for an aircraft engine to cool down to room temperature from the point it is turned off by the pilot?," Quora. [Online]. Available: https://www.quora.com/How-long-does-it-take-for-an-aircraft-engine-to-cool-down-to-room-temperature-from-the-point-it-is-turned-off-by-the-pilot. [Accessed on May 2021].